PRNU Enhancement Effects on Biometric Source Sensor Attribution

Luca Debiasi[1,*] and Andreas Uhl[1]

[1]Department of Computer Sciences, Jakob-Haringer-Str. 2, University of Salzburg, Salzburg, Austria
[*]ldebiasi@cosy.sbg.ac.at

Abstract: Identifying the source camera of a digital image using the photo response non-uniformity (PRNU) is known as camera identification. Since digital image sensors are widely used in biometrics, it is natural to perform this investigation with biometric sensors. In this paper we focus on a slightly different task, which consists in clustering images with the same source sensor in a data set possibly containing images from multiple unknown distinct biometric sensors. Previous work showed unclear results because of the low quality of the extracted PRNU. In this paper we adopt different PRNU enhancement techniques together with the generation of PRNU fingerprints from uncorrelated data in order to clarify the results. Thus we propose extensions of existing source sensor attribution techniques which make use of uncorrelated data from known sensors and apply them in conjunction with existing clustering techniques. All techniques are evaluated on simulated data sets containing images from multiple sensors. The effects of the different PRNU enhancement approaches on the clustering outcome are measured by considering the relation between cohesion and separation of the clusters. Finally an assessment on whether the PRNU enhancement techniques have been able to improve the results is given.

1. Introduction

Investigations in the field of digital image forensics usually comprise forensic tasks like device identification, device linking, recovery of processing history and the detection of digital forgeries. The photo response non-uniformity (PRNU) of an imaging sensor has emerged as an important forensic tool for the realisation of these tasks. Slight variations among individual pixels during the conversion of photons to electrons in digital image sensors are considered as the source of the PRNU; thus, it is an intrinsic property which forms an inherent part of all digital imaging sensors and their output, respectively. All digital image sensors cast this weak, noise-like pattern into each and every image they capture.

This systemic and individual pattern, which enables the identification of the image sensor itself, is essentially an unintentional stochastic spread-spectrum watermark that survives processing, such as lossy compression or filtering. Essential criteria like dimensionality, universality, generality, stability and robustness [1] make it well suited for forensic tasks, as the ones mentioned before. The identification of a digital image sensor can be performed at different levels as described by Bartlow *et al.* [2]: technology, brand, model, unit. In this work we focus on the unit level, which corresponds to a distinction of sensor instances of the same model and brand. For the purpose of sensor identification, a so called *PRNU fingerprint* can be calculated from multiple images of the same sensor, which is considered to be more robust for this task than a single image.

Besides the application of the PRNU for forensic tasks in general, it can also be useful in a biometric context. A biometric sensor's PRNU can also be used to improve a biometric system's security by ensuring the authenticity and integrity of images acquired with the biometric sensor deployed in the system. Previous work by Höller *et al.* [3] performed a feasibility study on the CASIA-Iris V4 database. They investigated the differentiability of the sensors in the CASIA-Iris V4 database by exploiting their PRNU and concluded that the equal error rates (EERs) and respective thresholds fluctuate considerably, depending on the sensor. Other work by Kalka *et al.* [4] regarding the differentiability of iris sensor showed varying results as well, while studies conducted on fingerprint sensors by Bartlow *et al.* [2] showed more satisfactory results.

The question raised, that if PRNU fingerprints are being applied as an authentication measure for biometric databases, the reason for the poor differentiation results for some sensors has to be investigated. On one hand it was assumed that this high variation could be caused by the correlated data that was used to generate the sensor's PRNU fingerprint, since all images investigated in [3] have a very similar image content. On the other hand, Kalka *et al.* [4] concluded that the variations are caused by the absence of the PRNU in saturated pixels (pixel intensity $= 255$) or under saturated pixels (pixel intensity $= 0$) for different images in the data sets. Furthermore Höller *et al.* [3] suspected that multiple sensors may have been used for the acquisition of the CASIA-Iris V4 subsets. If a PRNU fingerprint is generated using images of different sensors, it will match images acquired with all of these sensors and hence lead to a decreased differentiability. Other factors that negatively have negative effects on the differentiability are non-unique artifacts (NUAs) [5] and other high frequency components of the images, such as textured image content or edges. Several techniques to attenuate PRNU contaminations have been proposed in the literature [6, 7, 8, 9, 10, 11, 12].

For the previously mentioned sensor identification task the PRNU fingerprints are usually pre-calculated using images from sensors available to the investigators. However when we think about a realistic scenario, this availability is not always given. The images under investigation could be part of an image set containing images from an unknown number of different cameras. Before an image source identification can be performed in this scenario, images acquired with the same camera need to be identified and grouped together first. This task is known as source camera attribution in an open set scenario [13] or source camera clustering. Several clustering techniques have already been suggested by other researchers, who performed Hierarchical Agglomerative Clustering (HAC) [14, 15] or Multi-Class Spectral Clustering (MCSC) [13] for this scenario by formulating the classification task as a graph partitioning problem. Other related work by Bloy [16] relies on an iterative algorithm that progressively agglomerates images with similar PRNU using a pre-calculated threshold function to generate a PRNU fingerprint for the sensor. Some of the source sensor attribution techniques used in [17] are used in this work together with the previously mentioned approach of Bloy [16] and the source camera attribution techniques proposed in [14], [18] and [15]. The size of the extracted PRNU for consumer cameras used for source sensor attribution found in literature ranges from a very small size of 128×128 [15], 256×512 [14], 640×480, [19] to full size images of several Megapixels, where the most common size appears to be 1024×1024 [16, 20]. The results reported for consumer cameras show that the size of the extracted PRNU plays a major role for the performance of the various techniques, where plausible results can be obtained with PRNU patches larger than 1024×1024 pixels in general and 256×512 pixels using additional PRNU enhancements.

In this work, we conduct a source sensor attribution on different biometric data sets from different biometrics modalities, which aims at determining whether the images in the data sets described

in Section 4 have been acquired using multiple instances of the same sensor model. The investigation is conducted without taking any a priori knowledge about the sensors into consideration. To improve the quality of the extracted PRNU, we make use of various PRNU enhancement techniques which aim at attenuating undesired artefacts in the extracted PRNU as described in Section 2. Furthermore, additional uncorrelated data acquired with the same sensors as utilised to acquire the data sets is used for the generation of high-quality PRNU fingerprints. The performance of using the high-quality PRNU fingerprints is compared to the application of the various PRNU enhancement techniques. We propose novel extensions of the previously mentioned source sensor attribution techniques in Section 3 to be able to make use of the uncorrelated data. Section 5 explains the experimental set-up and describes the measure used for the evaluation of the clustering outcome and also contains the discussion of the experimental results. Finally Section 6 concludes the paper.

This work is an extended version of a paper previously published in [21]. We extend our previous work by proposing additional source sensor attribution techniques that make use of uncorrelated data from known sensors and measure their performance on simulated data sets containing images from multiple sensors and different PRNU sizes as well as on existing biometric data sets mostly containing an unknown number of source sensors. Furthermore a quantitative assessment on the effects of using data from known sensors compared to various PRNU enhancement approaches and the combination of both of them is given based on a metric measuring the cohesion and separation of the clustering result for each technique.

2. PRNU Extraction and Enhancement

The extraction of the photo response non-uniformity (PRNU) noise residuals is performed by applying Fridrich's approach [22]. For each image I the noise residual W_I is estimated as described in Equation (1),

$$W_I = I - F(I) \tag{1}$$

where F is a denoising function filtering out the sensor pattern noise. In this work we made use of four different denoising algorithms: The two wavelet-based denoising filters proposed by Lukas *et al.* in Appendix A of [23] (F_{Luk}) and Mihcak *et al.* in [24] (F_{Mih}), the BM3D denoising filter proposed by Dabov *et al.* [6] (F_{BM3D}) and the FSTV algorithm proposed by Gisdolf *et al.* [9] (F_{FSTV}).

After the PRNU extraction the noise residual W_I may be contaminated with undesired artefacts. In order to attenuate their effects different PRNU enhancement techniques have been proposed in the literature. Zero-meaning of the noise residuals's pixel rows and columns (*ZM*) removes NUAs with regular grid structures as described in [22]. Li [7] developed a technique for attenuating the influence of scene details or textured image content on the PRNU so as to improve the device identification rate of the identifier. This approach is referred to as *Li*. According to Lin *et al.* [12] some components of the extracted PRNU noise residual are severely contaminated by the errors introduced by denoising filters. They proposed a filtering distortion removal (*FDR*) algorithm that improves the quality of W_I by abandoning those components. The extracted and enhanced PRNU noise residual for a sample image using the various denoising filters and PRNU enhancements can be seen in Figure 1.

Finally the PRNU noise residual W_I is normalised in respect to the L_2-norm because its embedding strength is varying between different sensors as explained by [3].

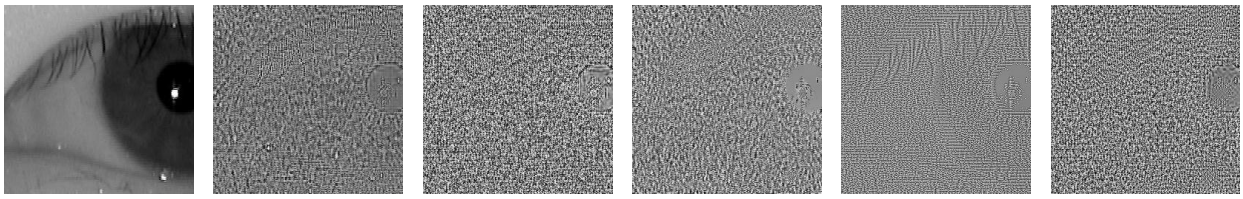

a b c d e f

Fig. 1. *Comparison of different denoising filters and PRNU enhancements applied to a cropped iris image from the* H100_2013 *data set.*
a Original image
b F_{Luk}+*ZM*
c F_{Luk}+*Li*
d F_{BM3D}
e F_{FSTV}
f F_{Mih}+*FDR*

The PRNU fingerprint (PRNU FP) $\hat{K}$ of a sensor is then estimated using a maximum likelihood estimator for images I_i with $i = 1...N$.

$$\hat{K} = \frac{\sum_{i=1}^{N} W_I^i I_i}{\sum_{i=1}^{N} (I_i)^2} \tag{2}$$

PRNU fingerprints can be contaminated with NUAs as well. To further enhance the quality of PRNU fingerprints a Wiener filtering (*WF*) applied in the Discrete Fourier Transform (DFT) domain is proposed in [1] to suppress periodic artefacts. Lin *et al.* [11] proposed a novel scheme named spectrum equalisation algorithm (*SEA*), where the magnitude spectrum of the PRNU fingerprint K is equalised through detecting and suppressing the peaks according to the local characteristics, aiming at removing the interfering periodic artefacts.

A method to detect the presence of a specific PRNU fingerprint in an image which has not been geometrically transformed is the normalised cross correlation (NCC), which is defined in Equation (3).

$$NCC(A,B) = \frac{\sum_{w=1}^{W}\sum_{h=1}^{H}(A(w,h)-\overline{A})(B(w,h)-\overline{B}))}{\sqrt{(\sum_{w=1}^{W}\sum_{h=1}^{H}(A(w,h)-\overline{A})^2)(\sum_{w=1}^{W}\sum_{h=1}^{H}(B(w,h)-\overline{B})^2)}} \tag{3}$$

A and B are two matrices of the same size $w \times h$ and $\overline{A}$ and $\overline{B}$ is their respective mean. The mean of a matrix X with size $w \times h$ is defined as:

$$\overline{X} = \frac{1}{WH}\sum_{w=1}^{W}\sum_{h=1}^{H} X(w,h) \tag{4}$$

The normalised cross correlation (NCC) is used to detect the presence of a PRNU fingerprint $\hat{K}$ in an Image I with

$$\rho_{[I,\hat{K}]} = NCC(W_I, I\hat{K}) \tag{5}$$

where ρ indicates the correlation between the noise residual W_I of the image I and the PRNU fingerprint $\hat{K}$ weighted by the image content of I.

On the other hand, the NCC can also be used to measure the similarity of two PRNU noise residuals $\hat{W}_I$ and $\hat{W}_J$ from two sensors S_i and S_j, as shown in Equation 6.

$$\rho_{[\hat{W}_I, \hat{W}_J]} = NCC(\hat{W}_I, \hat{W}_J) \tag{6}$$

Fridrich [1] proposed an alternative technique for measuring the similarity of two PRNU noise residuals or a PRNU noise residual and a PRNU FP, the Peak Correlation Energy (PCE), which has proven to be yield more stable results in a scenario where the images have been subject to geometrical transformations, such as rotations or scaling. Since all images used in this work have not undergone any of these transformations and Kang *et al.* showed that PCE by definition may increase the false positive rate in [25], we decided to use the NCC over the PCE.

3. Source Sensor Attribution Techniques

In this work we consider various techniques for the source sensor attribution task, where we apply various existing source attribution techniques and propose a novel one. We furthermore propose novel extensions for these existing methods for the case that the sensor is available to the investigators and uncorrelated data is used to generate the PRNU fingerprint. The uncorrelated data is generated by acquiring images with high saturation (but not over saturated) and smooth content, according to Fridrich [1]. All the mentioned clustering techniques generate a list of clusters, where the association of each image in the investigated data set to a cluster and thus a cluster label is obtained. The novel extensions of the existing methods together with a brief explanation of the original techniques are given in the following section.

3.1. (KS)BCF

In [16] Bloy proposed the Blind Camera Fingerprinting and Image Clustering (BCF) technique, which performs an agglomerative clustering to construct PRNU fingerprints from a mixed set of images, enabling identification of each images source camera without any prior knowledge of source. This technique solely depends on a pre-calculated threshold function. Using this threshold function t an automatic clustering algorithm performs the following steps:

1. Randomly select pairs of images until a pair is found whose noise correlation exceeds $t(1)$; average the PRNU of this pair to form a fingerprint.
2. Perform the first pass: for each remaining image, correlate the PRNU with the fingerprint. When the correlation value exceeds t(# of images in fingerprint cluster), average (cluster) it into the fingerprint. When $n = 50$ images have been averaged into the fingerprint or all images have been tried, stop and go to Step 3.
3. Perform the second pass: loop over all the unclustered images a second time, correlating with the current fingerprint and adding those that exceed the threshold. (Do not average more than 50 images into the fingerprint but allow more than 50 to be associated with the fingerprint.)
4. Repeat Step 1. Stop when Step 1 has tried 1000 pairs without success.

To be able to use the uncorrelated data, the first step (Step 1) is modified so that during the first iteration a PRNU Fingerprint is calculated from the uncorrelated data and the selection of two random images is skipped. After this modified step each remaining image is compared to this fingerprint as described in Step 2 and 3. After comparing all images, Step 1 is repeated as in the

original algorithm by selecting two random images. We call this extension *Known Sensor Blind Camera Fingerprinting and Image Clustering* (KSBCF), as noted in the original paper [21].

3.2. (KS)SWx

The Sliding Window Fingerprinting (SW) technique proposed in [26] consists of a so called "sliding window" with an arbitrary but fixed size n that moves over a data set image by image. This forensic technique uses an iterative algorithm which performs the following steps:

1. Start at image with index $i = 0$.
2. Gather images inside the sliding window with size n, hence the images with index $i \dots i + n$.
3. Extract the PRNU noise residual for each image.
4. Compute a PRNU fingerprint using the images inside the window.
5. Increment the index i by 1.
6. Repeat step 2 until all the images have been used to calculate a PRNU fingerprint.

Moving the window over the whole data set yields a list of PRNU fingerprints, which have been computed using sequential overlapping windows. For a data set containing m images, $m-n$ PRNU fingerprints are generated. After generating the fingerprints, the similarity of a PRNU fingerprint FP_i from the iteration i with all other fingerprints FP_j where $i \neq j$ is computed by calculating the NCC score of each fingerprint pair. This leads to a similarity matrix with size $(m - n) \times (m - n)$ containing all the pairwise NCC scores. The NCC scores of the PRNU FP comparisons where the FPs contain at least one common image are set to 0 because their correlation score would be much higher than average and introduce a bias to the clustering.

In the original paper [26] the number of clusters is determined in an explorative way by observing changes of the correlation scores. This leads to a rather vague estimation of the cluster structure in the data set. Hence, to assess the underlying cluster structure in a quantitative manner, we propose to apply different existing clustering techniques to cluster the obtained similarity matrix of pairwise PRNU fingerprint comparisons. In this work we applied the Unsupervised Clustering of Digital Images (UCDI) [14], the Fast Image Clustering (FIC) [15] and finally the Multi-Class Spectral Clustering (MCSC) algorithm [18]. The lower case "x" in the technique name indicates the applied clustering technique: *U* for UCDI, *F* for FIC and *M* for the MCSC technique.

These techniques yield a list of clusters and the PRNU fingerprints associated to each cluster. To obtain a cluster association for each image in the data set instead of each generated PRNU FP, we perform a majority voting based on the images used to generate each PRNU FP and the cluster association: Each image is used for the generation of multiple PRNU FPs because of the sliding window property, hence we count the cluster association frequency of the PRNU FPs, which contain the specific image, and select the highest cluster label occurrence as the final decision for the image. This gives a cluster label for each image in the data set.

For the *Known Sensor Sliding Window Fingerprinting* (KSSWx) a PRNU fingerprint is calculated with the uncorrelated data and is added to the list of PRNU FPs generated from the data set. This leads to a similarity matrix with size $(m - n + 1) \times (m - n + 1)$. This similarity matrix is again clustered using the previously mentioned UCDI, FIC and MCSC clustering techniques.

3.3. (KS)KM

For this source sensor clustering technique Lloyd's K-Means clustering algorithm [27] (KM) has been adopted, as previously proposed in [17]. K-Means is a vector quantisation method for cluster analysis used in data mining that partitions n objects into k clusters. The centroid for each cluster

Table 1. *List of simulated and existing biometric data sets used in this work with additional information. "SI" denotes the number of distinct sensor units used for acquiring the images in each data set.*

Type	Data set name	# Images	Sensor Model	Image Size	SI	Sensor Type
Simulated	*SIMeven*	450	Various Consumer Cameras	$\geq 3264 \times 2448$	3	Digital Camera
	SIMuneven	450	Various Consumer Cameras	$\geq 3264 \times 2448$	3	Digital Camera
	SIMdominant	450	Various Consumer Cameras	$\geq 3264 \times 2448$	3	Digital Camera
Existing	*H100_2009*	908	Irisguard H100 IRT	640×480	?	Iris Sensor
	H100_2013	1451	Irisguard H100 IRT	640×480	1	Iris Sensor
	IPH_2009	1620	OKI Irispass-h	640×480	?	Iris Sensor
	IPH_2013	970	OKI Irispass-h	640×480	1	Iris Sensor
	URU_1	1000	Digital Persona UrU4000 #1	328×356	1	Fingerprint Sensor
	URU_2	1000	Digital Persona UrU4000 #2	328×356	1	Fingerprint Sensor

is the point to which the sum of distances from all objects in that cluster is minimised which leads to a set of clusters that are as compact and well-separated as possible. We define the PRNU noise residuals of the images in the investigated data set as the n objects to cluster, while k is the number of different sensors (clusters). Because the number of sensors for some data sets is unknown we repeated the clustering for $k = 1 \ldots 5$ with the assumption that not more than 5 sensors have been used. This limitation is not mandatory and can be extended if necessary, but increases the computational effort significantly.

We propose an extension of this technique, the *Known Sensor K-Means Clustering* (KSKM), to be able to make use of the uncorrelated data. We first generate a PRNU FP from the uncorrelated data, which is then added to the set of PRNU noise residuals n which is clustered. Additionally we select this generated PRNU FP as starting point for the algorithm together with $k-1$ random other samples from the data set. We repeat the K-Means algorithm 5 times with the computed PRNU FP and $k-1$ randomly chosen samples as starting points to avoid the possibility to get stuck in local minima and the clustering of the best run out of these 5 is selected as final result.

4. (Biometric) Data Sets

First of all, we generated simulated data sets to examine the performance of the source sensor attribution techniques presented in Section 3. These data sets all consist of images from 3 distinct sensors from a popular Sensor Forensics benchmark database, the Dresden Image Database [28]: Agfa DC-830i, Panasonic DMC-FZ50 and Nikon D200. The data sets all contain randomly selected images from each sensor, where we shuffled chunks of 50 images to obtain a random order. We then generated three different data set types based on the frequency of images from each of the 3 sensors:

- *SIMeven*: 150 images from each sensor.
- *SIMuneven*: 200 images from the first, 150 from the second and 100 from the third sensor.
- *SIMdominant*: 350 images from one sensor and 50 from the two others each.

We repeated the data set generation 10 times for each of the three simulated data set types, where the sensors' order for the image distribution is determined randomly each time, e.g. the sensors

providing the most images in the *SIMdominant* data set was chosen randomly each time.

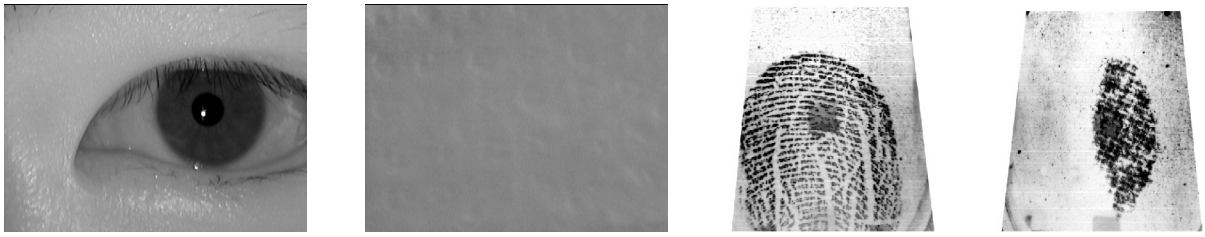

a b c d

Fig. 2. *Sample images from data sets with additionally acquired uncorrelated data for the corresponding sensor. The "Digital Persona UrU4000" sensor prevented the acquisition of images without containing at least a partial imprint.*
a Image from *H100_2009*.
b Uncorrelated data acquired with Irisguard H100 IRT iris sensor.
c Image from *URU_2*.
d Uncorrelated data acquired with Digital Persona UrU4000 #2 fingerprint sensor.

The existing biometric data sets under investigation in this work consist of images for two different biometric modalities, iris and fingerprints, which are illustrated in Table 1 together with the simulated ones. These biometric data sets have not been published; however, the iris data sets ending with "2013" and fingerprint ones "URU_1" and "URU_2" have been acquired during a COST Short Term Scientific Mission (STSM) as described in [29], while data sets ending with "2009" have been provided by the host institution during the mentioned COST STSM. The ground truth on the number of sensor instances used for the acquisition is only known for the *H100_2013*, *IPH_2013*, *URU_1* and *URU_2* data sets, which consists of 1 sensor instance. For all other data sets only the sensor model is known, but not how many instances of this model have been used.

All images in this work are 8 bit grey-level JPEG files. The iris data has been collected under near infrared illumination, while the fingerprint sensors used red LEDs. The uncorrelated data used in this work to acquire the PRNU fingerprints for the known sensors has been acquired according to [29] for the following sensors: *OKI Irispass-h*, *Irisguard H100 IRT*, *Digital Persona UrU4000 #1* and *Digital Persona UrU4000 #2*.

To obtain high-quality PRNU fingerprints as described by Fridrich in [1], images with uncorrelated content and high saturation have been acquired. In some cases the sensor's quality assessment prevented the acquisition of such images, therefore the acquisition was performed in a best effort approach by varying the image content as much as possible to gain a "cleaner" PRNU fingerprint when averaging the images. Figure 2 shows exemplary iris and fingerprint images from the existing data sets described above and uncorrelated data acquired with the same sensor. It points out a successful acquisition for the *Irisguard H100 IRT* sensor, and a less successful one for the *Digital Persona UrU4000 #2* sensor.

5. Experimental Set-up and Results

In the following Section we discuss the results of applying the various source sensor attribution techniques illustrated in Section 3 to the data sets in Section 4. First we explain the general experimental set-up, which contains a description of the methodology and parameters valid for all

experiments. After that we characterise the different experiments conducted in this work, which are divided into two different subsections, 5.1 and 5.2.

All the data sets described in Section 4 are investigated independently. The PRNU noise residuals are extracted from a square patch located in the center of each image. After the extraction the PRNU noise residuals are enhanced using one or more of the techniques mentioned in Section 2. For all clustering techniques where a PRNU fingerprint is generated, in addition PRNU fingerprint enhancements are also applied. The configuration of both enhancement types is described at the beginning of each experiment later on.

For the (KS)BCF and (KS)SWx only clusters containing 10 or more images are considered for the final number of clusters results. These techniques are prone to generate a few very small clusters for small PRNU sizes which would have a strong impact on the results because of the overall rather small number of clusters and furthermore, in the investigated biometric scenario, the case that such a small number of images in the data sets is acquired with a different sensor is highly unlikely.

In order to be able to quantitatively assess the clustering of the data sets and reveal differences caused by the various PRNU enhancement techniques the Mean Silhouette Value (MSV) by Rousseeuw [30] has been calculated for each source sensor attribution techniques clustering outcome.

The silhouette value for each point is a measure of how similar that point is to points in its own cluster, when compared to points in other clusters, hence it is a measure between intra- and inter-cluster distances. This technique does not rely on any ground truth information about the clustering of the investigated data set and is therefore well suited for our investigation because the ground truth is not known for all data sets used in this work, which can be seen in Table 1. The result for a single cluster, or $k = 1$, has been determined by calculating the pairwise NCC between all point combinations i and j, where $i \neq j$, and then calculating the mean correlation over all points. For all $k >= 2$ the Mean Silhouette Value for the i-th point, S_i, is defined as

$$MSV = \frac{1}{N} \sum_{n=1}^{N} \frac{b_i - a_i}{max(a_i, b_i)} \tag{7}$$

where N is the number of noise residuals, a_i is the average distance from the i-th point to the other points in the same cluster as i (cohesion), and b_i is the minimum average distance from the i-th point to points in a different cluster (separation), minimised over all clusters. The silhouette value ranges from -1 to $+1$. A high silhouette value indicates that a point i is well-matched to its own cluster, and poorly-matched to neighbouring clusters. If most points have a high silhouette value, then the clustering solution is considered to be an appropriate solution. On the other hand, if many points have a low or negative silhouette value, then the clustering solution may have either too many or too few clusters.

This concludes the general experimental set-up and we will now continue with the discussion of the experimental results for the *Simulated Data Sets*.

5.1. Simulated Data Sets

The performance evaluation of the source sensor attribution techniques is an important part of this work, since the effects of the advanced PRNU enhancement techniques evaluated later are assessed using the clustering outcome of the different techniques. Hence we applied the various clustering techniques on the simulated data sets *SIMeven*, *SIMuneven* and *SIMdominant*. The

PRNU is extracted with the basic *ZM+WF* configuration, which uses the F_Luk denoising filter, enhances the noise residuals with *(*ZM) and the PRNU fingerprints with *ZM+WF* according to [22].

We measure the performance of the proposed source sensor attribution techniques on the simulated data sets for varying PRNU patches (square size): 64, 128, 256, 512, 768, 1024, 1536 and 2048 pixels. In this case the resulting scores and number of clusters are averaged over the 10 different randomly generated data sets of each data set type (*SIMeven*, *SIMuneven* and *SIMdominant*) separately.

For the simulated data sets, where the ground truth on the source sensor for each image is known, we compute the V-Measure (VM) [31] score for the clustering outcome, which is defined as harmonic mean of homogeneity (h) and completeness (c) as shown in Equation (8).

$$VM = 2 * \frac{h * c}{h + c} \qquad h = 1 - \frac{H(C|K)}{H(C)} \qquad c = 1 - \frac{H(K|C)}{H(K)} \tag{8}$$

The homogeneity h measures whether each cluster exclusively contains images from the same sensor, while the completeness c measures if all images belonging a sensor have been assigned to the same cluster. $H(C|K)$ refers to the conditional entropy of the different classes for the given cluster associations and $H(C)$ denotes the entropy of the classes. Further details can be found in the corresponding paper [31].

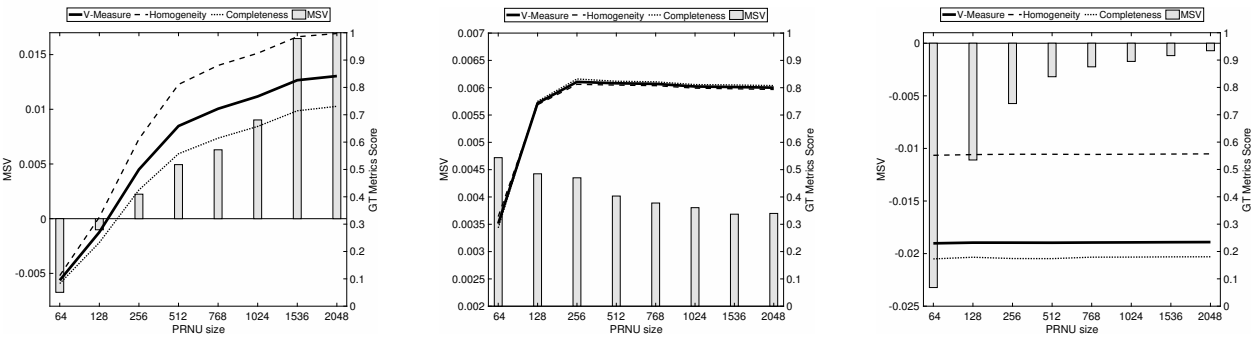

Fig. 3. *Averaged Mean Silhouette Values (MSV) and computed ground truth (GT) metrics (V-Measure, Homogeneity, Completeness) examples for three different source sensor attribution techniques applied to the simulated data sets* SIMeven*,* SIMuneven *and* SIMdominant *using different sizes for the extracted PRNU and the basic* ZM+WF *PRNU enhancement configuration. The scores have been averaged over the three data sets.*
a BCF.
b KM.
c SWF.

First of all we have a look at how the size of the extracted PRNU affects the performance. Since the simulated data sets contain higher resolution images than the biometric data we are able to test various extracted PRNU sizes from 64×64 to 2048×2048 pixels. The results show that the VM scores increase proportionally with the PRNU size for some techniques, where BCF shows a steady increase in clustering performance with increasing PRNU size, while for KM the performance increases until a certain point and then stagnates. The stagnation of the VM scores after a certain PRNU size occurs due to the the technique's inability to further exploit the additional

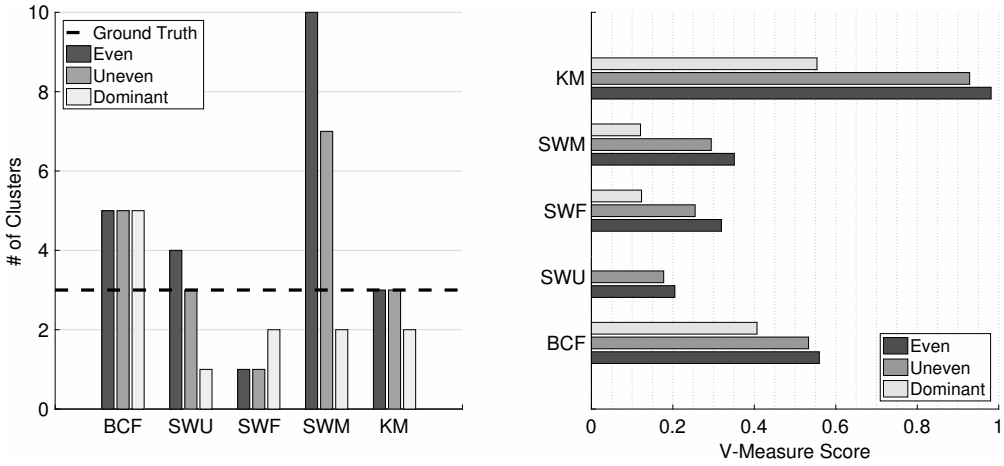

Fig. 4. *Resulting number of clusters (right) and V-Measure scores (left) for each of the source sensor attribution techniques applied on the simulated data sets using a* 256×256 *pixel PRNU patch size and the basic* ZM+WF *PRNU enhancement configuration. The expected number of sensors used to create the data sets (*3*) is shown as the dashed line (Ground Truth).*

data for the differentiation of the sensors in the data. Thus it reaches a point where additional data does not change the cluster association of the images.

The MSV scores in general increase with larger PRNU size, except for the KM technique. The decreasing MSV scores for the KM technique with larger PRNU sizes can be explained by how the MSV scores are calculated. For the MSV scores we consider pairwise Euclidean distances between the PRNU noise residuals, which become more and more inaccurate with increasing dimensionality (i.e. PRNU size), as shown in [32]. Due to the cluster association staying the same for larger PRNU sizes, the MSV scores decrease because of this effect in higher dimensions. For the SWx techniques the MSV score increases with higher dimension because of their inability to cluster the data properly.

For the SWx techniques the VM performance is consistently bad across all tested PRNU sizes. The reason for this are the very low homogeneity scores for the SWU, the very low completeness scores for SWF and while SWM shows the best VM score of the three, but suffers from both mediocre homogeneity and completeness scores. The VM and MSV results for BCF, KM and SWF are illustrated in Figure 3.

Due to the limit of the biometric data to extract the PRNU from a 256×256 patch we compared the performance of all techniques with this configuration, which can be seen in Figure 4. It shows that the highest VM score is obtained by the KM technique, which shows a high score for the *SIMeven* and *SIMuneven* data sets, while it seems to struggle with the *SIMdominant* data set. In general all techniques obtain much lower scores for the *SIMdominant* data set with BCF being the only exception. Although the SWU and SWM generate a number of clusters close to the expected result of 3, the quality of the clusters in respect to the homogeneity and completeness is quite low. BCF on the other hand generates a few more clusters, but their quality is higher, which is indicated by the higher VM score.

Summarising the KM and BCF techniques are the most qualified techniques to cluster the data for the tested PRNU size. The KM technique obtains the highest scores for all three simulated data sets, but the performance varies highly depending on the distribution of the images from different sensors within the data sets. The BCF technique on the other hand performs worse than the KM

one due to being prone to produce more clusters, which is penalised by the VM measure. However the produced clusters all have a high homogeneity and by having the most consistent results across all the simulated data sets still consider this method as well suited for the clustering. Due to the poor results for the SWx techniques they can not be recommended for this kind of scenario, thus for the remaining evaluation only the BCF and KM techniques are taken into consideration.

5.2. Iris and Fingerprint Data Sets

In this section, *Iris and Fingerprint Data Sets*, we discuss the effects of applying different PRNU enhancement techniques on the existing biometric data sets. For these iris and fingerprint data sets we are only able to extract 256×256 pixel patches because of the varying image size to ensure the comparability of the results among all data sets.

The different configurations for the PRNU extraction process used for the experiments can be seen in Table 2. The parameters of all PRNU enhancement techniques have been chosen as recommended by the authors of the respective papers.

Table 2. *Enhancement configurations applied for the different steps of the PRNU extraction process. The abbreviations are explained in Section 2.*

Name	Denoising filter	Noise residuals	Fingerprints
ZM+WF [22]	F_{Luk}	ZM	WF
Li [7]	F_{Luk}	Li	-
BM3D [6]	F_{BM3D}	-	-
FSTV [9]	F_{FSTV}	-	-
FDR+SEA [12]	F_{Mih}	FDR+Li	SEA

This section is further divided into the following three subsections:

- In the *Baseline* subsection (5.2.1) we briefly evaluate the results obtained with the basic *ZM+WF* configuration applied for the PRNU extraction for all clustering techniques.
- The *PRNU Enhancements Side by Side* subsection (5.2.2) discusses the effects of the different PRNU extraction configurations applied for all clustering techniques.
- In the *Summary Biometric Data* subsection (5.2.3) we recapitulate the effects of the various PRNU extraction configurations and compare their performance across all data sets.

Before discussing the *Baseline* results, an overview over all results for the biometric data sets is given in Table 3, where we will depict some interesting observations in the following.

5.2.1. Baseline: The resulting MSV values relevant for the *Baseline* evaluation correspond to the *ZM+WF* rows of Table 3. The resulting clusters for all source sensor attribution techniques can be seen in Figure 5.

First of all we have a look at the iris and fingerprint data set results separately. The first thing we notice when looking at the iris data sets is that the BCF and KSBCF techniques produce a large number of clusters for the *IPH_2009* and *IPH_2013*, where both are not able to cluster the data properly. This is also confirmed by the negative MSV scores. However the use of uncorrelated

Table 3. *Mean silhouette values (MSVs) for the various combinations of PRNU enhancement configurations and source sensor attribution techniques. The numbers in parentheses show the ground truth number of clusters in the table header and the number of clusters generated for the different combinations of source sensor attribution techniques and data sets in the table body.*

		H100_2009 (?)	*H100_2013* (1)	*IPH_2009* (?)	*IPH_2013* (1)	*URU_1* (1)	*URU_2* (1)
BCF	ZM+WF	0.0161 (1)	0.0122 (1)	-0.0020 (6)	-0.0025 (6)	0.0035 (2)	0.0077 (2)
	Li	0.0171 (1)	0.0121 (1)	0.0024 (2)	0.0026 (2)	0.0065 (1)	0.0057 (2)
	BM3D	0.0197 (1)	0.0160 (1)	-0.0012 (2)	0.0011 (2)	0.0149 (1)	0.0115 (2)
	FSTV	-0.0401 (2)	-0.0004 (2)	-0.0002 (2)	0.0030 (2)	0.0095 (1)	0.0086 (2)
	FDR+SEA	0.0169 (1)	0.0120 (1)	-0.0009 (5)	0.0001 (4)	0.0139 (1)	0.0076 (2)
KSBCF	ZM+WF	0.0161 (1)	0.0122 (1)	-0.0015 (6)	-0.0019 (4)	0.0090 (2)	0.0088 (2)
	Li	0.0171 (1)	0.0121 (1)	0.0042 (1)	0.0095 (1)	0.0045 (2)	0.0051 (2)
	BM3D	0.0197 (1)	0.0160 (1)	0.0016 (2)	0.0023 (1)	0.0068 (2)	0.0101 (2)
	FSTV	-0.0660 (1)	0.0377 (1)	0.0019 (1)	0.0015 (1)	0.0044 (2)	0.0077 (2)
	FDR+SEA	0.0169 (1)	0.0120 (1)	0.0019 (5)	0.0008 (3)	0.0060 (2)	0.0066 (2)
KM	ZM	0.0161 (1)	0.0122 (1)	0.0036 (1)	0.0035 (1)	0.0291 (2)	0.0213 (2)
	Li	0.0171 (1)	0.0121 (1)	0.0207 (1)	0.0215 (1)	0.0242 (2)	0.0177 (2)
	BM3D	0.0197 (1)	0.0160 (1)	0.0214 (1)	0.0228 (1)	0.0414 (2)	0.0275 (2)
	FSTV	0.0344 (2)	0.0187 (1)	0.0230 (1)	0.0245 (1)	0.0347 (2)	0.0255 (2)
	FDR	0.0169 (1)	0.0120 (1)	0.0222 (1)	0.0233 (1)	0.0355 (2)	0.0259 (2)
KSKM	ZM+WF	0.0161 (1)	0.0122 (1)	0.0036 (1)	0.0035 (1)	0.0291 (2)	0.0213 (2)
	Li	0.0171 (1)	0.0121 (1)	0.0207 (1)	0.0215 (1)	0.0242 (2)	0.0177 (2)
	BM3D	0.0197 (1)	0.0160 (1)	0.0214 (1)	0.0228 (1)	0.0414 (2)	0.0275 (2)
	FSTV	0.0344 (2)	0.0187 (1)	0.0230 (1)	0.0245 (1)	0.0347 (2)	0.0255 (2)
	FDR+SEA	0.0169 (1)	0.0120 (1)	0.0222 (1)	0.0233 (1)	0.0355 (2)	0.0259 (2)

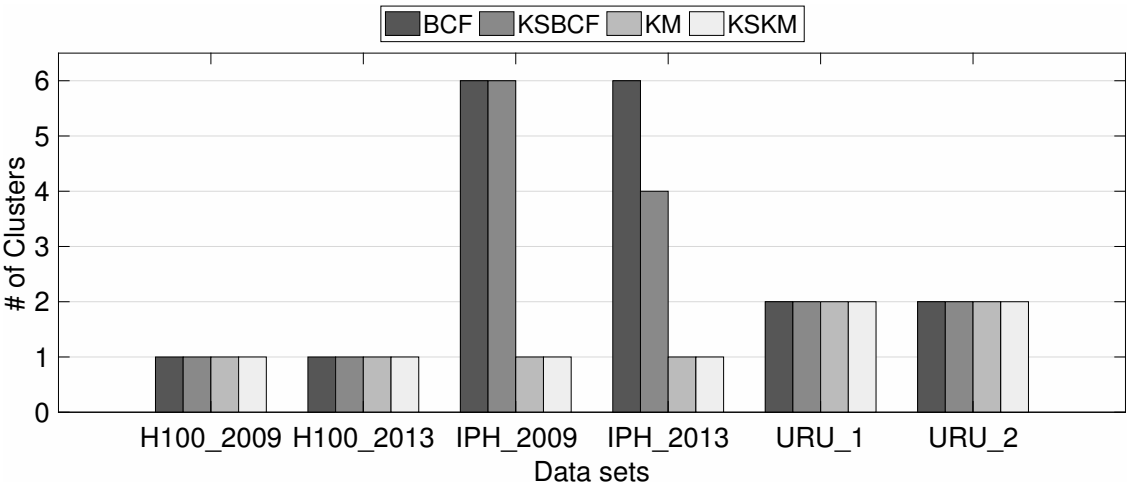

Fig. 5. *Clustering result with number of clusters for the* Baseline *evaluation (*ZM+WF*).*

data helps to improve the MSV scores slightly for KSBCF compared to BCF. KM and KSKM yield 1 cluster for all iris data sets, even for those with known ground truth that have been acquired with a single sensor. The use of uncorrelated data does not affect the MSV scores at all for the KSKM technique compared to KM.

For the fingerprint data sets *URU_1* and *URU_2* all clustering techniques fail at clustering the

data correctly and yield 2 clusters, even though the correct number would be 1. Yet all MSV scores are positive which indicates that the separation of the data into 2 clusters could be reasonable. The effects of the uncorrelated data are the same as for the iris data sets, where the MSV scores of KSBCF are slightly better than those for BCF and the MSV scores for KSKM do not show any change in comparison with KM.

5.2.2. PRNU Enhancements Side by Side: In this subsection we will have a look at the *Li*, *BM3D*, *FSTV* and *FDR+SEA* rows of Table 3, which contain the results of applying the PRNU extraction configurations described in Table 2. The evaluation of the results focuses on the BCF and KSBCF techniques first, followed by the KM and KSKM techniques.

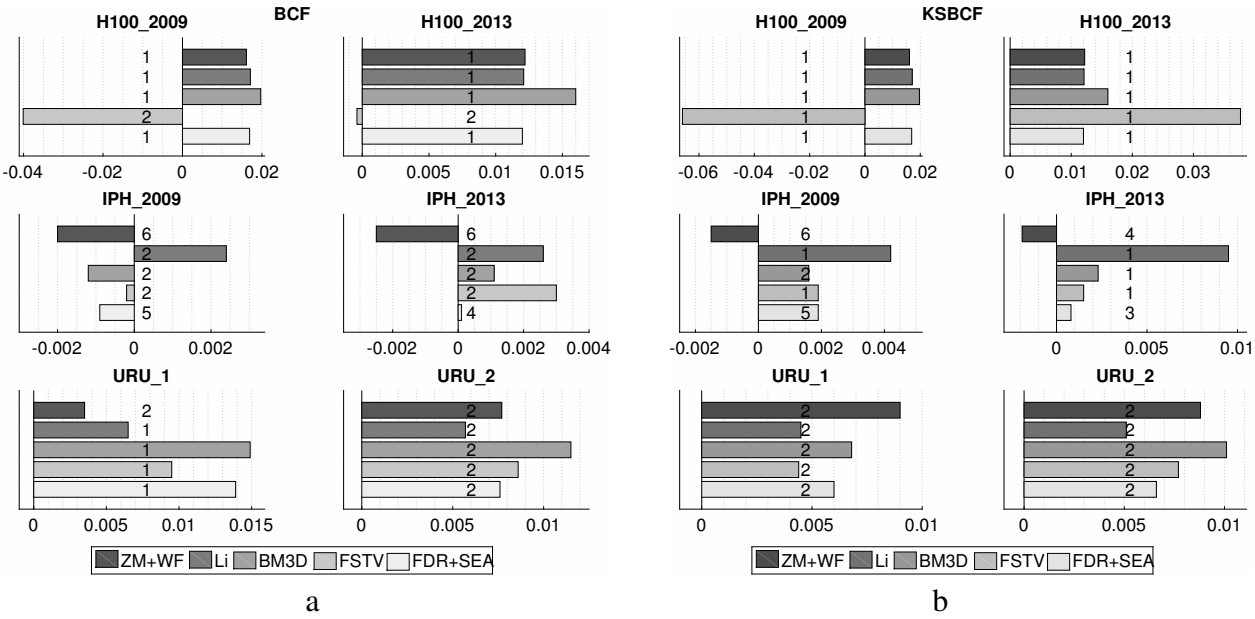

Fig. 6. *Comparison of number of clusters (at the center of each bar chart) and MSV values for the* Li*,* BM3D*,* FSTV *and* FDR+SEA *PNRU enhancement configurations compared to* ZM+WF *when applied in the BCF and KSBCF techniques.*
a BCF
b KSBCF

The results for the BCF and KSBCF techniques are graphically depicted in Figure 6. As we can see the BCF results for *H100_2009* and *H100_2013* are quite similar, where *BM3D* obtains the highest MSV scores. However all the other configurations are quite close with exception of *FSTV*, which yields an increased number of clusters (2) accompanied by negative MSV scores. The use of uncorrelated data in KSBCF has no effect on the MSV scores nor on the number of clusters for all configurations except FSTV, where it reduces the number of clusters to 1 in both data sets. The MSV scores for KSBCF and the FSTV configuration however are even further reduced for the *H100_2009*, while it shows a dramatic increase for the *H100_2013* data set where it even surpasses the previously best score of *BM3D* by a clear margin. The *IPH_2009* and *IPH_2013* have been very challenging for the basic *ZM+WF* and showed poor results due to the high number of clusters. All applied PRNU enhancement configurations show a MSV score improvement with all configurations for the BCF technique by decreasing the number of clusters even down to 2 in most cases. These results can be explained by the improved separability of the data due to the PRNU enhance-

ments. The best MSV score for *IPH_2009* is obtained by *Li*, while for *IPH_2013 FSTV* shows the highest MSV with the *Li* configuration being close. With the addition of uncorrelated data in KSBCF the number of clusters is decreased to 1 for some configurations in both data sets, which in the case of *IPH_2013* corresponds to the ground truth. *Li* takes the most advantage of these data and yields the by far highest MSV scores for both The *IPH_2009* and *IPH_2013* data sets. For the last two data sets, *URU_1* and *URU_2*, BCF is able to improve the MSV scores for almost all PRNU enhancement configurations. The number of clusters is decreased to 1 for *URU_1*, however for *URU_2* the number stays at 2, which is incorrect according to the ground truth. The highest MSV scores for both scores are obtained with the *BM3D* configuration. Interestingly the addition of uncorrelated data in KSBCF lowers the scores for all PRNU enhancement configurations compared to *ZM+WF*. Because the number of clusters remains constant, the the differentiability of the data could be negatively affected by the suboptimal capturing of the uncorrelated data for the fingerprint sensors, as shown in figure 2. *ZM+WF* yields the highest MSV score for *URU_1* and *BM3D* for *URU_2*.

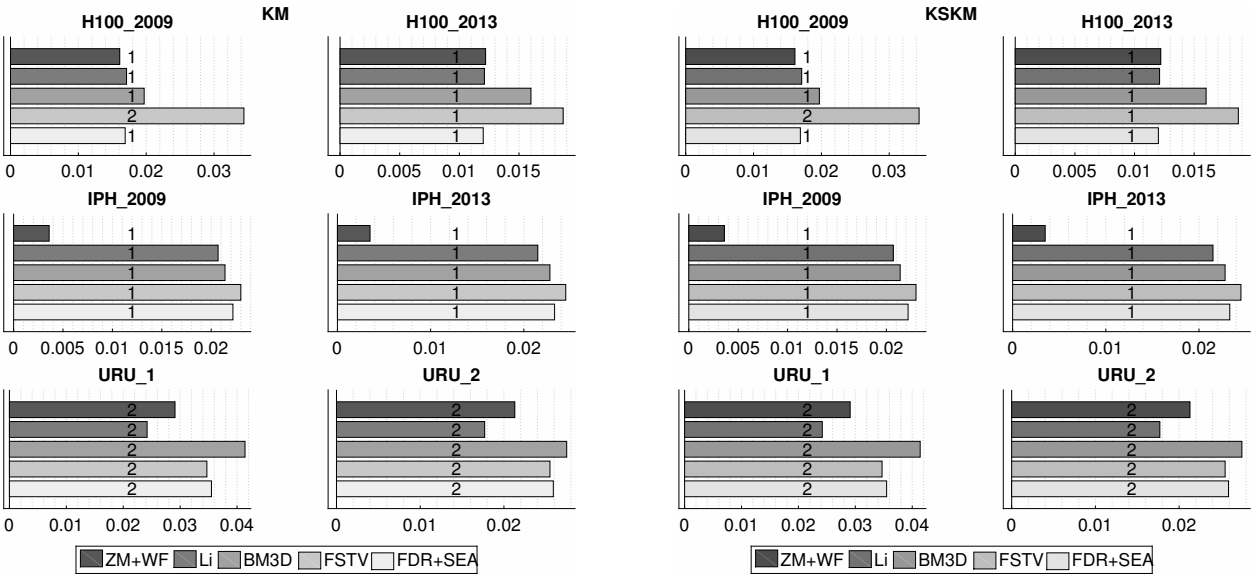

Fig. 7. *Comparison of number of clusters (at the center of each bar chart) and MSV values for the* Li*,* BM3D*,* FSTV *and* FDR+SEA *PNRU enhancement configurations compared to* ZM+WF *when applied in the KM and KSKM techniques.*
a KM
b KSKM

The second part of the evaluation looks at the results of the KM and KSKM clustering techniques, which are illustrated in Figure 7. The first thing that we notice here is that the use of uncorrelated data in the KSKM technique has absolutely no effect on the scores and number of clusters. Therefore all of the following statements relate to both KM and KSKM. In most cases the PRNU enhancement configurations show an improvement of the MSV scores, while not changing the resulting number of clusters. The only exception is *FSTV*, which increases the number of clusters to 2 for the *H100_2009* data set. The highest MSV scores for the iris data sets (*H100_2009*, *H100_2013*, *IPH_2009* and *IPH_2013*) are obtained by *BM3D* and by *FSTV* for the fingerprint data sets (*URU_1* and *URU_2*).

5.2.3. Summary Biometric Data: The preceding results for the biometric show that the adoption of the different PRNU enhancement configurations did indeed help to improve the clustering outcome of the clustering techniques. Figure 8 shows the PRNU enhancement configurations resulting in the highest MSV scores for each technique and data set. We can see that for the KM and KSKM technique *FSTV* is the best choice for the iris and *BM3D* for the fingerprint data sets. Regarding the BCF and KSBCF the choice of PRNU enhancement configuration is dependent on the data set or rather on the sensor model: For the data sets using the *Irisguard H100 IRT* sensor *BM3D* is the configuration of choice, while for the *OKI Irispass-h* sensor it is the *Li* configuration.

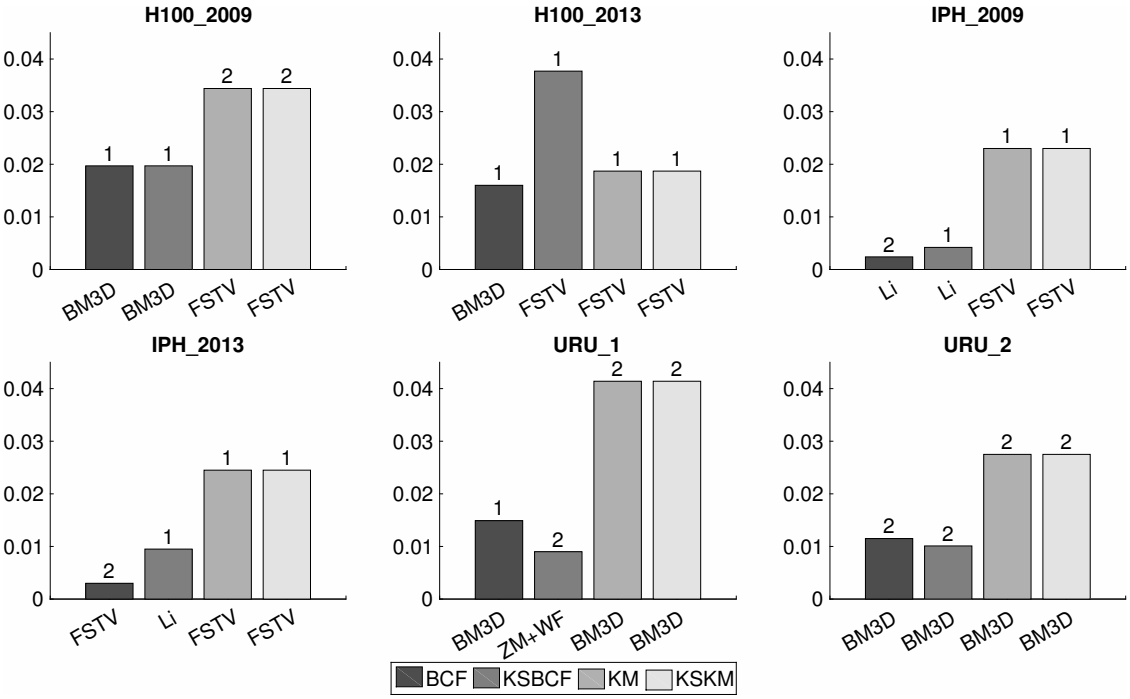

Fig. 8. *Highest MSV scores, according number of clusters (above bars) and PRNU enhancement configuration achieving the score for all clustering technique and data set combinations.*

The additional use of uncorrelated data had a very large impact on the clustering outcome of the KSBCF techniques applied on the *IPH_2009* and *IPH_2013* data sets compared to BCF. However for the other data sets the impact was quite small and for KSKM the uncorrelated data had no impact at all. This can be explained by how the KSKM technique makes use of the uncorrelated data, in fact it is only used to create a starting point for the K-means algorithm which then nevertheless converges to the same cluster centroids as without using this additional data.

Concerning the data sets for which the ground truth is known, the correct number of clusters for all iris data sets could be determined at least by applying a combination of uncorrelated data and PRNU enhancements. In contrast, for the fingerprint data set the correct number could only be established in one case. In all the others the clustering techniques failed to do so even with any combination of uncorrelated data and PRNU enhancement.

Recapitulating we can say that there is no single best PRNU enhancement configuration for this scenario, yet it is highly situational which one should be chosen.

6. Conclusion

In this work we proposed novel source sensor attribution techniques based on the sensors PRNU and applied existing ones. We generated multiple simulated data sets containing images from multiple sensors taken from the Dresden Image Database and computed different clustering quality metrics to evaluate the proposed techniques. The results showed that the size of the extracted PRNU has a significant impact on the clustering result. Two of the techniques, BCF and KM, have been able to cluster the data properly and showed consistent and promising results in the case of 256×256 PRNU patch sizes and have been considered appropriate for the source sensor attribution of biometric sensors.

In the following all techniques have been applied to biometric data sets with low resolution images of two different biometric modalities, iris and fingerprints, to cluster the images according to their source sensor. Different PRNU enhancement techniques have been adopted in response to the special characteristics of biometric data, such as highly correlated data and contamination of the PRNU by the image content, in order to improve the clustering performance. Additionally we used uncorrelated data acquired with the sensors and proposed several extensions for already existing sensor attribution techniques to be able to use this uncorrelated data in conjunction with the source attribution techniques.

The evaluation of the various PRNU enhancement and uncorrelated data effects was conducted by means of a quantitative measure for the clustering outcome, that considers the cohesion and separation of the clusters without the need of any knowledge about the underlying cluster ground truth. Summarising the results it can be stated that most PRNU enhancements did indeed help to improve the clustering results compared to the original work in [21] by increasing the differentiability of the PRNU noise residuals. However we could not identify any single enhancement technique or combination that was able to improve the clustering outcome for all data sets alike, but the choice of the best performing technique is highly situational. Furthermore the clustering techniques in most cases did not succeed in determining the correct number of clusters for the fingerprint data sets, even with the support of the different PRNU enhancements techniques.

For the fingerprint data sets the absent PRNU enhancement effect and poor results clearly needs some further and deeper investigation. The insufficient quality of the extracted PRNU might be an issue in this case, either caused by the image content or by other contaminations or factors, e.g. the amount of denoising applied during the biometric sensor's processing of the acquired image. Since biometric sensors are often closed systems tailored to acquire a specific type of images, the identification of these issues is challenging. In conclusion certainly further studies have to be conducted in this manner in regard to the special requirements posed by biometric sensors and the data they produce. A fusion of the source sensor attribution techniques' clustering outcome will also be investigated in future work.

7. Acknowledgment

This work is partially funded by the Austrian Science Fund (FWF) under Project No. P26630 and partially supported by a COST 1106 Short Term Scientific Mission (STSM).

8. References

[1] J. Fridrich. Sensor defects in digital image forensics. In H.T. Sencar and N. Memon, editors, *Digital Image Forensics: There is more to a picture than meets the eye*, chapter 6, pages 179–218. Springer Verlag, 2012.

[2] N. Bartlow, N. Kalka, B. Cukic, and A. Ross. Identifying sensors from fingerprint images. In *Computer Vision and Pattern Recognition Workshops, 2009. CVPR Workshops 2009. IEEE Computer Society Conference on*, pages 78–84, June 2009.

[3] A. Uhl and Y. Höller. Iris-sensor authentication using camera PRNU fingerprints. In *Proceedings of the 5th IAPR/IEEE International Conference on Biometrics (ICB'12)*, pages 1–8, New Delhi, India, March 2012.

[4] N. Kalka, N. Bartlow, B. Cukic, and A. Ross. A preliminary study on identifying sensors from iris images. In *The IEEE Conference on Computer Vision and Pattern Recognition (CVPR) Workshops*, June 2015.

[5] T. Gloe, S. Pfennig, and M. Kirchner. Unexpected artefacts in prnu-based camera identification: a 'dresden image database' case-study. In *MM&Sec'12: Proceedings of the 14th ACM Multimedia and Security Workshop*, pages 109–114. ACM, September 2012.

[6] K. Dabov, A. Foi, V. Katkovnik, and K. Egiazarian. Image denoising by sparse 3-d transform-domain collaborative filtering. *Image Processing, IEEE Transactions on*, 16(8):2080–2095, 2007.

[7] Ch.-T. Li. Source camera identification using enhanced sensor pattern noise. *IEEE Transactions on Information Forensics and Security*, 5(2):280–287, 2010.

[8] A. J. Cooper. Improved photo response non-uniformity (prnu) based source camera identification. *Forensic Science International*, 226(13):132 – 141, 2013.

[9] F. Gisolf, A. Malgoezar, T. Baar, and Z. Geradts. Improving source camera identification using a simplified total variation based noise removal algorithm. *Digital Investigation*, 10(3):207 – 214, 2013.

[10] X. Kang, J. Chen, K. Lin, and P. Anjie. A context-adaptive spn predictor for trustworthy source camera identification. *EURASIP Journal on Image and Video Processing*, 2014(1):19, 2014.

[11] X. Lin and Ch.-T. Li. Preprocessing reference sensor pattern noise via spectrum equalization. *IEEE Transactions on Information Forensics and Security*, 11(1):126–140, 2016.

[12] X. Lin and Ch.-T. Li. Enhancing sensor pattern noise via filtering distortion removal. *IEEE Signal Processing Letters*, 23(3):381–385, 2016.

[13] I. Amerini, R. Caldelli, P. Crescenzi, A. Del Mastio, and A. Marino. Blind image clustering based on the normalized cuts criterion for camera identification. *Signal Processing: Image Communication*, 29(8):831–843, 2014.

[14] Ch.-T. Li. Unsupervised classification of digital images using enhanced sensor pattern noise. In *ISCAS*, pages 3429–3432. IEEE, 2010.

[15] R. Caldelli, I. Amerini, F. Picchioni, and M. Innocenti. Fast image clustering of unknown source images. In *IEEE International Workshop on Information Forensics and Security (WIFS) 2010*, pages 1–5, 2010.

[16] G. Bloy. Blind camera fingerprinting and image clustering. *IEEE Transactions on Pattern Analysis and Machine Intelligence*, 30(3):532–534, March 2008.

[17] L. Debiasi and A. Uhl. Techniques for a forensic analysis of the casia-iris v4 database. In *Proceedings of the 3rd International Workshop on Biometrics and Forensics (IWBF'15)*, 2015.

[18] B. b. Liu, H. K. Lee, Y. Hu, and C. H. Choi. On classification of source cameras: A graph based approach. In *Information Forensics and Security (WIFS), 2010 IEEE International Workshop on*, pages 1–5, Dec 2010.

[19] E.J. Alles, Z.J.M.H. Geradts, and C.J. Veenman. Source camera identification for low resolution heavily compressed images. In *Proceedings of the 2008 International Conference on Computational Science and Its Applications, ICCSA '08), Special Session on Computational Forensics, COMPFOR '08*, Perugia, Italy, June 2008.

[20] I. Amerini, R. Becarelli, B. Bertini, and R. Caldelli. Acquisition source identification through a blind image classification. *IET Image Processing*, 9(4):329–337, 2015.

[21] L. Debiasi and A. Uhl. Comparison of prnu enhancement techniques to generate prnu fingerprints for biometric source sensor attribution. In *Proceedings of the 4th International Workshop on Biometrics and Forensics (IWBF'16)*, pages 1–6, Limassol, Cyprus, 2016.

[22] J. Fridrich. Digital image forensic using sensor noise. *IEEE Signal Processing Magazine*, 26(2), March 2009.

[23] J. Lukas, J. Fridrich, and Miroslav Goljan. Digital camera identification from sensor pattern noise. *IEEE Transactions on Information Forensics and Security*, 1(2):205–214, 2006.

[24] M. Mihcak, I. Kozintsev, and K. Ramchandran. Spatially adaptive statistical modeling of wavelet image coefficients and its application to denoising. In *Proceedings of the 1999 IEEE International Conference on Acoustics, Speech, and Signal Processing, ICASSP '99*, pages 3253–3256, Phoenix, AZ, USA, March 2009. IEEE.

[25] X. Kang, Y. Li, Z. Qu, and J. Huang. Enhancing source camera identification performance with a camera reference phase sensor pattern noise. *IEEE Transactions on Information Forensics and Security*, 7(2):393–402, 2012.

[26] L. Debiasi and A. Uhl. Blind biometric source sensor recognition using advanced prnu fingerprints. In *Proceedings of the 2015 European Signal Processing Conference (EUSIPCO 2015)*, 2015.

[27] S.P. Lloyd. Least square optimization in PCM. *IEEE Transactions on Information Theory*, 2(IT-28):129–137, March 1982.

[28] T. Gloe and R. Bhme. The dresden image database for benchmarking digital image forensics. In *SAC 2010: Proceedings of the 2010 ACM Symposium on Applied Computing*, pages 1584–1590. ACM, 2010.

[29] L. Debiasi, Z. Sun, and A. Uhl. Generation of iris sensor PRNU fingerprints from uncorrelated data. In *Proceedings of the 2nd International Workshop on Biometrics and Forensics (IWBF'14)*, 2014.

[30] P. Rousseeuw. Silhouettes: A graphical aid to the interpretation and validation of cluster analysis. *J. Comput. Appl. Math.*, 20(1):53–65, November 1987.

[31] A. Rosenberg and J. Hirschberg. V-measure: A conditional entropy-based external cluster evaluation measure. In *Proceedings of the 2007 Joint Conference on Empirical Methods in Natural Language Processing and Computational Natural Language Learning(EMNLP-CoNLL)*, pages 410–420, 2007.

[32] C. C. Aggarwal, A. Hinneburg, and D. A. Keim. On the surprising behavior of distance metrics in high dimensional space. In *Lecture Notes in Computer Science*, pages 420–434. Springer, 2001.